https://doi.org/10.1016/j.coco.2023.101496

Ultrafast-responsive Carbon Nanotube-grafted Fibre Textiles

Yiyin Su[a, b, §], Hanmo Zhou[c, d, §], Xishan Guo[a, e], Yinfei Zheng[a, f], Xiaohui Yang[a], Haitao Huang[d], Li-min Zhou[c], and Zhongqing Su[b, *]

[a]Research Center for Humanoid Sensing, Zhejiang Lab, Hangzhou, PR China

[b]Department of Mechanical Engineering
The Hong Kong Polytechnic University, Kowloon, Hong Kong SAR

[c]School of System Design and Intelligent Manufacturing
Southern University of Science and Technology, Shenzhen, PR China

[d]Department of Applied Physics
The Hong Kong Polytechnic University, Kowloon, Hong Kong SAR

[e]Department of Biosystems Engineering
Zhejiang University, Hangzhou, China

[f]Department of Biomedical Engineering, Biosensors National Special Lab
Zhejiang University, Hangzhou, China

Submitted to ***Composites Communications***
(Initially submitted on 25th Oct 2022, revised and re-submitted on 1st Jan 2023)

§ These authors contributed equally to this work.
* To whom correspondence should be addressed. Tel.: +852-2766-7818, Fax: +852-2365-4703;
Email: zhongqing.su@polyu.edu.hk (Prof. Zhongqing Su, *Ph.D.*)

Abstract

Direct grafting of carbon nanotubes (CNTs) on fibre textiles is a promising strategy to functionalize conventional fibre-reinforced polymer composites with extra merits such as integrated sensing capability. In this study, CNTs are *in situ* grafted on glass fibre (GF) via chemical vapor deposition at a low synthesis temperature (500 ℃). By regulating the mass fractions of CNTs, the quantum tunnelling effect can be triggered among CNT nanoparticles, with which the CNT-grafted GF textiles manifest high sensitivity to structure-guided ultrasonic waves in a frequency regime from 175 to 375 kHz. With ignorable degradation in mechanical attributes due to this direct grafting processing as affirmed by ASTM-complied tests (ASTM C1557 and D3039), the CNT-grafted GF textiles demonstrate the great potential in developing hybrid functional composites.

Keywords**:** structural health monitoring; guided ultrasonic waves; structural integrity monitoring; chemical vapor deposition

1. Introduction

Direct grafting carbonaceous nanomaterials, particularly carbon nanotubes (CNTs) on fibres broadens the applications of conventional fibre-reinforced polymer composites (FRPs) in structural health monitoring (SHM) [1], electromagnetic interference shielding [2], lighting strike protection [3], *etc.* Prevailing grafting techniques, as represented by dip coating [4], spray coating [5], and electrophoretic deposition [6], are a solution-based deposition process, in which a homogenous CNT suspension is prerequired. To achieve this, chemical surfactants and organic polymers are usually adopted. However, the residues of these additives on fibre surfaces may weaken mechanical properties and etch fibres [7]. Additionally, these approaches provide random distribution of CNTs with a low density, which only results in slight improvement in targeted properties.

In contrast, chemical vapor deposition (CVD) owns the great potential to control the orientation, alignment, and loading of deposited CNTs, providing the possibility to tailor the properties of composites [3, 5, 8]. The synthesized CNTs form a nanostructured buffer interphase at the interface of fibre and matrix, relieve stress concentration induced by the mismatch in mechanical properties of fibre and matrix, and improve the bonding strength. Luca *et al.* [9] demonstrated that the uniform CNTs increased the interfacial shear strength by 12%, as measured in the single fibre pull-out test. Though great achievements in enhancing interfacial properties have been achieved via direct growing CNTs on fibres, a challenging issue that the harsh CVD process generally sacrifices the mechanical strength of fibres still exists. Luca *et al.* [9] synthesized CNTs on high silica glass fibres at 760 °C, with which the tensile strength of fibres significantly decreased from 4.15 to 2.15 GPa, by 48.2%, due to the excessive exposure to high temperature.

On the other hand, when grafting CNTs on dielectric fibres (*e.g.*, glass, basalt, and sisal), the inherent piezoresistivity of thus-networked CNTs endows hybrid composites with the sensing capability. Sebastian *et al.* [10] showed that fuzzy CNT-decorated GF sensors exhibited similar gauge factors

(1.6–2.3) to standard strain gauge (~2.0) and responded to stimuli at longitudinal, transverse, and off-axis directions. He *et al.* [7] also interpreted the electrical resistance (ER) variation measured by CNT-coated glass fibres (GFs) in the flexural test, showing that the ER increased in a stepwise manner with the applied strain. Nonetheless, most reported studies in the similar vein are constrained to ER-based sensing domain, which only provides qualitative and holistic estimation between measured electrodes, and fails to detect the damage away from sensors.

Distinguished from conventional ER-based measurement, sensing and scrutinizing high-frequency guided ultrasonic waves (GUWs), propagating in host composite structures, can quantitatively provide structural status information, as GUWs carry and accumulate rich information along the propagation path [11, 12]. However, most proposed embedded nanocomposite-based sensors fail to respond to ultrasonics due to their characteristics of high frequency and ultralow magnitude [13].

In this study, a genre of sensing fibre textile, developed from direct grafting CNTs on GF textiles via CVD, is presented to sense high-frequency dynamic strains (*e.g.*, ultrasonics), which can further fulfill GUW-based structural integrity monitoring (SIM) of composite structures. Detailed interrogations are conducted on the morphology and quality of synthesized CNTs. The density of grafted CNTs is regulated to promote the quantum tunnelling effect and endow the sensing fibre textiles with appropriate responsivity towards GUWs, along with analysis of the perception mechanism. Tensile tests at two scales, namely the single fibre tensile test (ASTM C1557) and fibre-reinforced polymer matrix composite tensile test (ASTM D3039), are carried out to investigate the possible influence of proposed CVD technique on the tensile attributes.

2. Materials and Methods

2.1 Materials

Plain weave E-glass fibre textiles (High Gain® 175 gsm) are applied as the reinforcement while the selected matrix consists of epoxy resin (WEST SYSTEM® 105) and hardener (WEST SYSTEM® 209). Analytical grade ethanol (Honeywell® 24194) is adopted as both the hydrocarbon precursor for the growth of CNTs and the solvent for the catalyst precursor (cobalt (II) nitrate hexahydrate supplied by International Laboratory®), and the 5 vol% H_2/N_2 gas mixture (LINDE®) is simultaneously used as the reducing and carrier gas for the proposed CVD process.

2.2 Grafting of CNTs on Fibre Textiles

The cobalt (II) nitrate hexahydrate is dissolved in ethanol to formulate a sprayable catalyst precursor suspension with a concentration of 5.0 wt.%, followed by being sonicated in an ultrasonic bath for two hours to facilitate the dissolution of solute. The as-received GF textiles are pre-covered with a polyimide molding film with elaborately designed hollowed-outs, at which the catalyst precursor is deposited during the spraying of aqueous suspension to initiate the growth of CNTs in the sequent CVD process.

The catalyst precursor-deposited textiles are rolled up and then inserted into the quartz tube of a furnace. Prior to the heating starts, an inert environment is created via thoroughly purging the gas mixture. The tube is heated to 450 ℃ (with a rate of 10 ℃/min) and maintained at this temperature for 30 mins to reduce the catalyst precursor in a hydrogen-maintained atmosphere. The temperature continuously elevates to 500 ℃, to initiate the growth of CNTs while the ethanol vapor (at 85 ℃) is introduced into the tube via shifting the flow path of gas mixture from Path 1 to Path 2, schematically depicted in **Fig. 1**, to provide the carbon source for the growth of CNTs. The synthesisation of CNTs lasts for 30 mins. The appropriate selections of hydrocarbon source, catalyst precursor, and carrier gas, which differentiate this study from other works, lead to the direct growth of CNTs at a low

temperature.

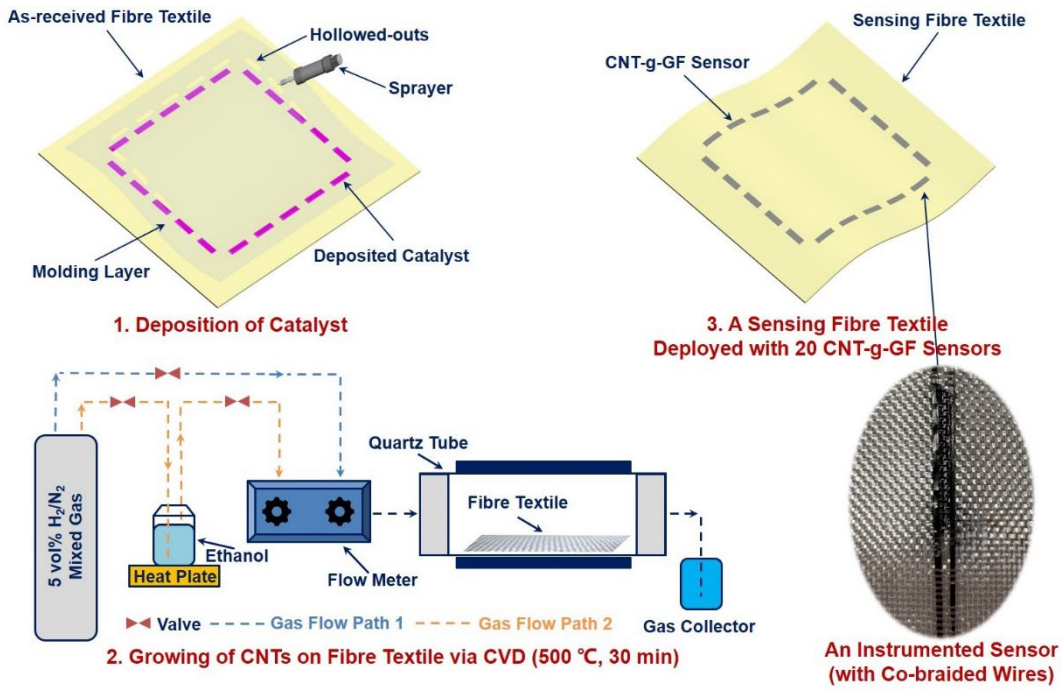

Fig. 1. Preparation flowchart of sensing fibre textile deployed with CNT-grafted GF sensors.

2.3 Characterization

The morphology of CNT-grafted GF, referred to as CNT-g-GF hereinafter, is first investigated on a scanning electron microscopy (SEM) platform (TESCAN® MAIA3). Thermogravimetric analysis (TGA, Mettler Toledo® TGA/DSC 3+) is performed to quantify the mass fraction of CNTs, with the total mass of CNT-g-GF as a reference. The prepared CNT-g-GF specimens are heated from 25 to 800 ℃ at a rate of 10 ℃/min in an air-purging (50 sccm) atmosphere. The Raman spectra of synthesized CNTs are acquired with a Raman spectrometer (WItec® alpha300R, λ = 532 nm) to evaluate their quality while their tubular structure is revealed on a transmission electron microscopy (TEM) platform (JEOL® JEM-2011).

With the method described in Section 2.2, CNTs are initiated to grow at 20 targeted regions of a GF fabric, each of which will be configured as a sensor with a planar dimension of 30 × 2 mm^2, to make a sensing textile. Highly conductive CNT-film (DexMat®) are braided into the sensing textile, to connect the sensors with the signal acquisition system, shown in **Fig. 1**. The linear resistance of the

CNT-film-made wires is only ~20 Ω per meter in length and 1 mm in width, guaranteeing well signal transmission. 20 thus-developed sensors configure a sensor network in a square fashion, with a side length of 300 mm. Such-made sensing textile is then laid up, as the 4th ply, together with another seven plies of as-received fabrics, to fabricate an 8-ply orthotropic laminate (500 × 500 × 1.15 mm^3) via the vacuum-assisted resin transfer molding (VARTM) technique, which imposes a high pressure to indent the CNT-film-made wires into CNT-grafted GF sensors, ensuring a good conductive connection but without the need of electrodes.

To interrogate the responsivity of the sensing textile layer to high-frequency GUWs, an ultrasonic measurement system is configured. To emit GUWs into the laminate, a home-made PIN-PMN-PT single crystal-based transducer, which is configured with a parylene matching layer to enhance the transmitting sensitivity, is surface-glued at the centre of the laminate. 5-cycle Hanning-function-modulated sinusoidal tonebursts are generated with a waveform generator and applied on the PZT wafer, after amplified to 400 V_{pp} via a linear power amplifier (Ciprian® US-TXP-3).

Two categories of tensile tests, namely the single fibre tensile test (ASTM C1557) and fibre-reinforced polymer matrix composite tensile test (ASTM D3039), are launched to scrutinize the influence of proposed CVD process and grafted CNTs on tensile properties, with the detailed description of these two experiments provided in the supplementary material.

3. Results and Discussion

3.1 Basic Characteristics of CNTs

Through regulating the amount of deposited catalyst precursor, which is achieved via spraying different volumes of catalyst precursor suspension on textiles in this work, fibre textiles are grafted with CNTs of six representative loadings. As can be visually inspected in **Fig. 2(a)**, the colour of CNT-g-GFs gradually gets darker with increasing loading of CNTs. The TGA curves demonstrate

that the representative mass fractions of CNTs are 0.38 wt.%, 0.45 wt.%, 0.64 wt.%, 0.81 wt.%, 0.85 wt.%, and 1.07 wt.%, in **Fig. 2(b)**. **Fig. 2(c)** provides the Raman spectra of CNT-g-GFs with mass fractions of 0.64 wt.%, 0.81 wt.%, 0.85 wt.%, and 1.07 wt.%. The peak, positioned at ~1340 cm^{-1}, is known as the D-band corresponding to disorder structure while the G-band locating at ~1580 cm^{-1} represents the sp^2 carbon-formed graphitic structure. To quantify the quality of synthesized CNTs, the I_d/I_g ratio is calculated. For the investigated four categories, their I_d/I_g ratios are all less than 0.89, indicating the high degree of graphitization. The TEM image, in **Fig. 2(d)**, reveals the co-axial, thin-walled tubular structure of CNT. The morphologies of CNT-g-GFs with various mass fractions are exhibited in **Fig. 3**, which will be discussed in detail along with their responsivities to GUWs in the sequent section.

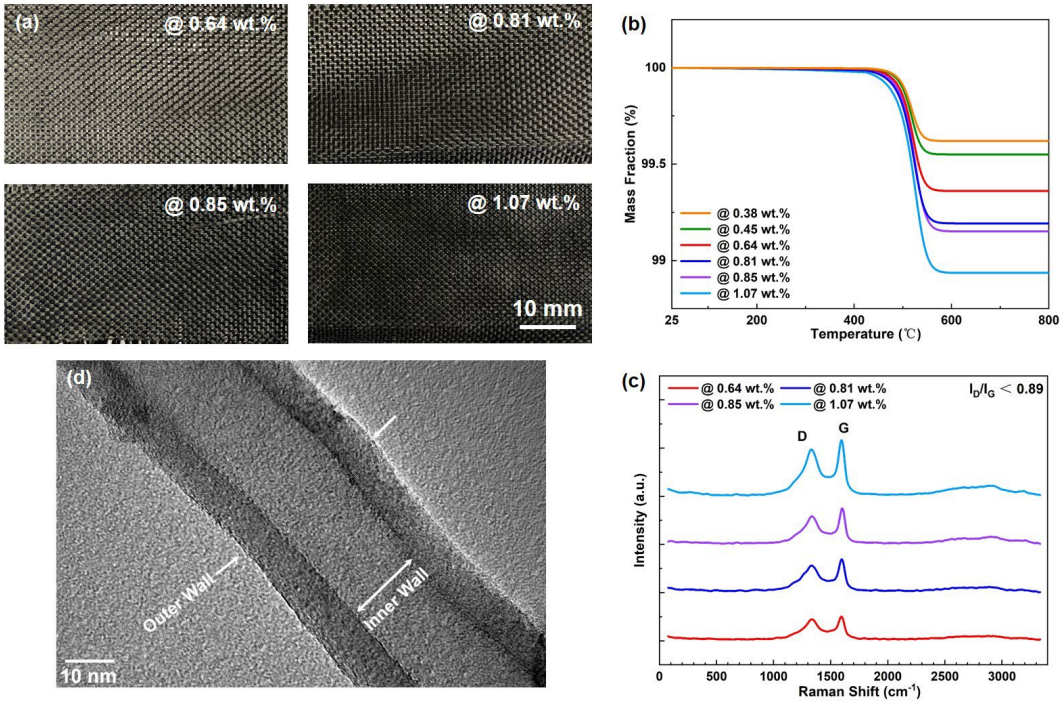

Fig. 2. (a) Photograph of; (b) TGA curves of CNT-g-GFs, with various mass fractions of CNTs; (c) Raman Spectra of CNT-g-GFs; and (d) TEM image of a synthesized CNT.

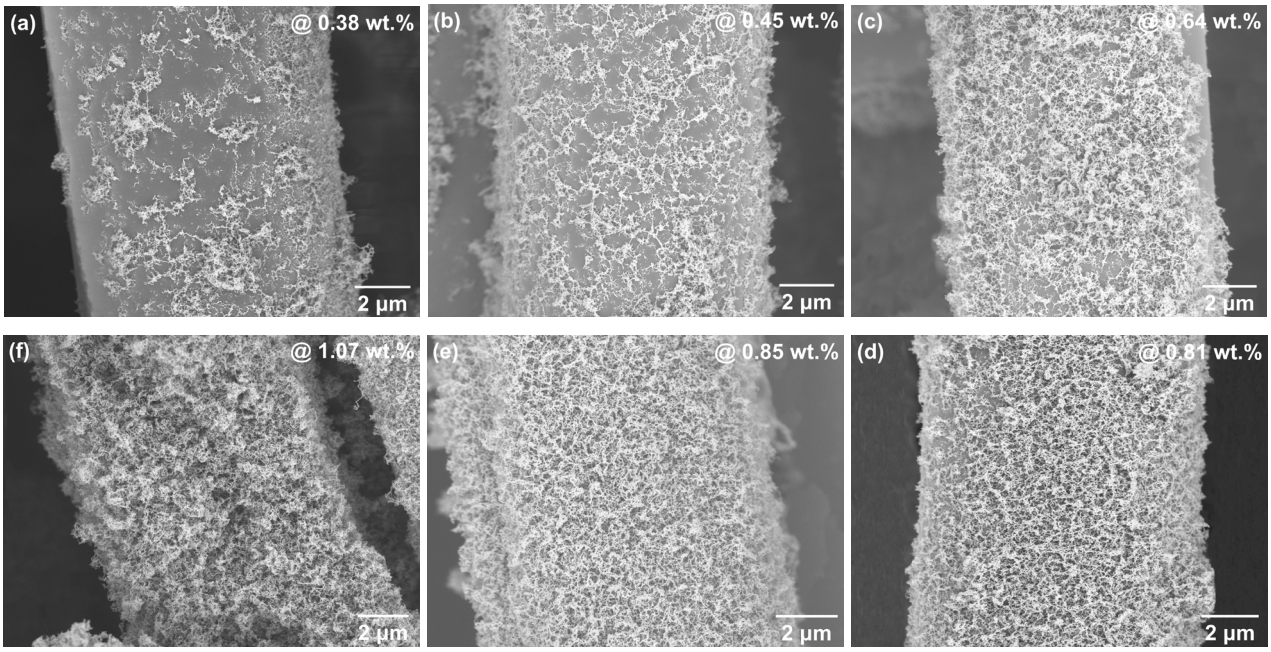

Fig. 3. SEM images showing the morphologies of CNT-g-GFs with different CNT loadings.

3.2 Response to Guided Ultrasonic Waves

The ER of conductive CNT networks (R) embraces three key components, namely the intrinsic resistance of conductive CNTs (R_{CNT}), the contact resistance ($R_{Contact}$) owing to direct contact among adjacent CNTs and the tunnelling resistance ($R_{Tunnelling}$) induced by the tunnelling effect. It has been concluded that GUWs generally induce microstrains, which are insufficient to cause destruction of conductive pathways (*e.g.*, separation or loss of contacts of CNT nanoparticles) and lead to measurable variation in $R_{Contact}$ [14]; on top of that, the change in R_{CNT} can be neglected due to the superb conductivity of CNTs. To acquire appropriate sensitivity of CNT-g-GF sensors towards GUWs, it is therefore essential to promote the variation in $R_{Tunnelling}$ and trigger the tunnelling effect when GUWs disturb the CNT-g-GF sensors. On the other hand, the quantum tunnelling effect is particularly prominent when the nanoparticles, synthesized CNTs in this work, are in close proximity with others [15]. With such a sensing philosophy, the synthesized CNTs are far preferable to be distributed in a close but not direct contact manner, which can be achieved via regulating the mass fraction of grafted CNTs.

To put the investigation into perspective, **Fig. 4** compares signals, at representative 175 kHz, captured by CNT-g-GF sensors with various loadings of CNTs, observing different response sensitivities. All perceived signals are pre-averaged 1024 times to minimize measurement uncertainty and subsequently filtered with a first-order Butterworth filter to mitigate ambient noise. To specify, with sparse CNTs (@ 0.38 wt.%), the conductive pathways are discontinuous, **Fig. 3(a)**, showing non-responsiveness to dynamic strains, in **Fig. 4(a)**. With gradually increased loadings (@ 0.45 wt.%, 0.64 wt.%), the CNTs come into contact or are in close proximity with neighboring particles to stimulate the piezoresistivity of CNT networks and CNT-g-GF sensors at these two mass fractions demonstrate responsiveness to GUWs, though relatively weak. Such a phenomenon is attributed to that as can be observed in **Figs. 3(b)** and **(c)**, there still exist some bare regions on the GF surface, indicating insufficient formation of conductive pathways. With appropriate mass fractions of CNTs (@ 0.81 wt.%, 0.85 wt.%), the GFs are fully and evenly grafted with CNTs, forming adequate electron transmission paths, **Figs. 3(d)** and **(e)**. GUW-induced strains alter the distance of adjacent CNTs, trigger the tunnelling effect and lead to remarkable variation in $R_{Tunnelling}$, providing high sensitivity towards GUWs, **Figs. 4(d)** and **(e)**. At the weight ratio of 1.07 wt.%, the CNT-g-GF sensor exhibits a reduced sensitivity to GUWs, **Fig. 4(f)**. That is because at such a loading, the majority of CNTs are distributed in a contact manner, **Fig. 3(f)**, CNTs entangle and agglomerate one with the other, which suppresses the variation in ER manifested by the sensors, when GUWs introduce dynamic strains to CNT-g-GFs.

To further scrutinize the sensing performance of CNT-g-GF sensors (@ 0.85 wt.%), **Fig. 5** comprehensively depicts their responses towards ultrasonics with a frequency regime from 200 to 375 kHz, arguing that such sensors are capable of precisely capturing dynamic strains with a high signal-to-noise ratio.

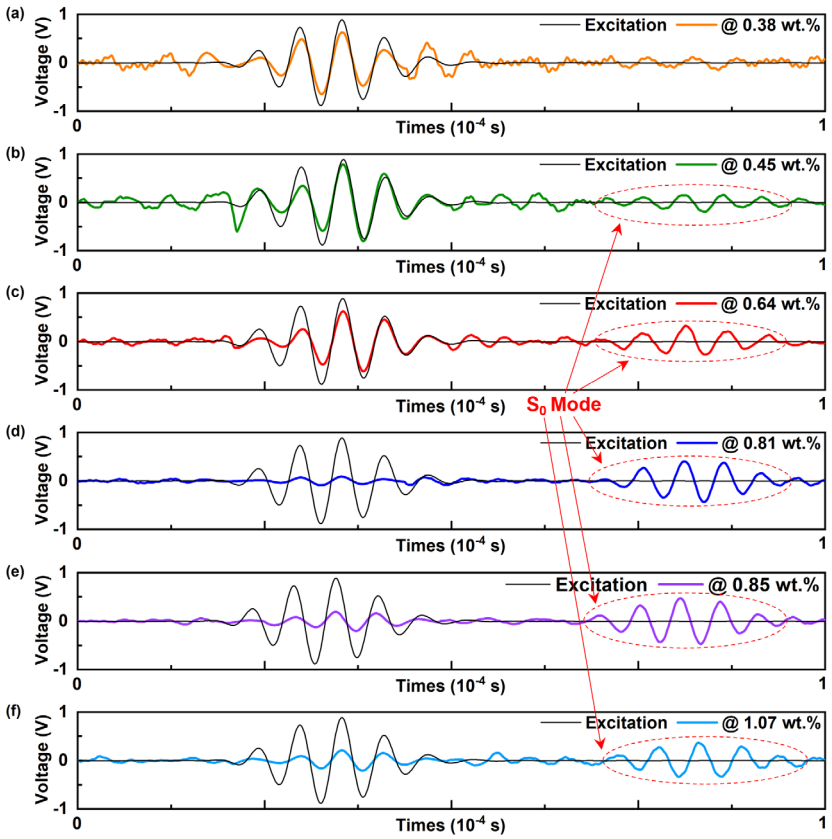

Fig. 4. Signals captured by CNT-g-GF sensors with different CNT loadings, at 175 kHz.

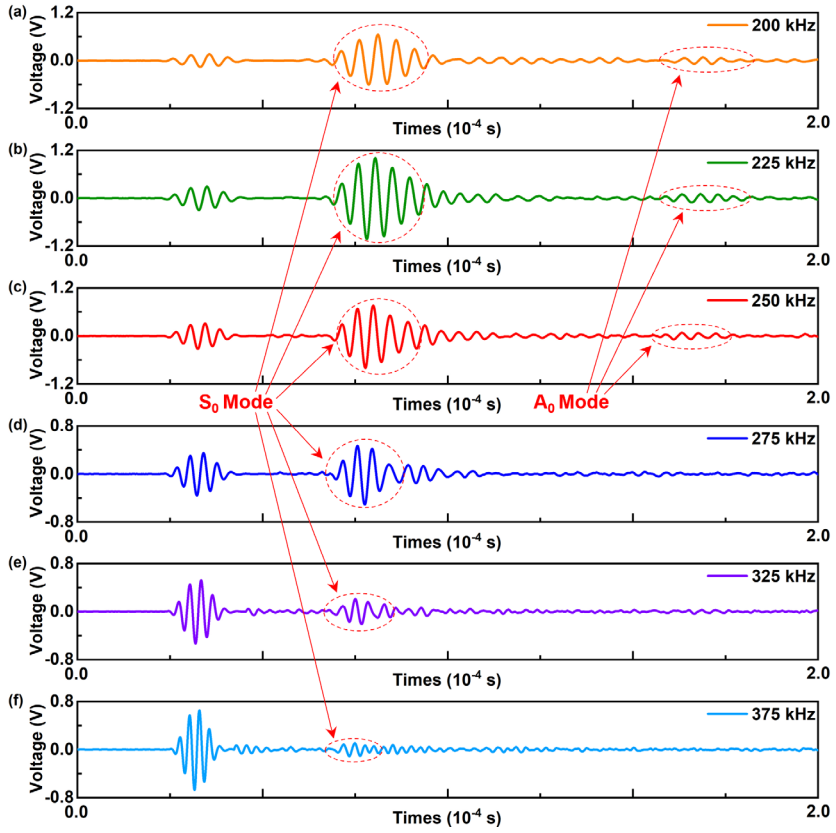

Fig. 5. GUW signals captured by CNT-g-GF sensors @ 0.85 wt.%, in a frequency regime from 200 to 375 kHz.

3.3 Tensile Properties

The Weilbull statistical method is recalled to analyse the results of single fibre tensile test, for assessing the axial properties of glass fibres with or without grafted CNTs. The tensile strength of fibre can be determined as

$$\sigma = \frac{4F}{\pi d_f^2}, \quad \textbf{(1)}$$

where F is the force to failure and d_f the fibre diameter. The scattered distribution of the single fibre tensile results shown in **Fig. 6(a)**, acquired with both the as-received GFs and the CNT-g-GFs @ 0.85 wt.%, can be attributed to the high variability characteristic of the single fibre tensile test approach. With two-parameter Weibull distribution [16, 17], the experimental data are analysed using

$$F(\sigma) = 1 - \exp\left(-L(\sigma/\sigma_0)^{\beta_W}\right), \quad \textbf{(2)}$$

where $F(\sigma)$ is the failure probability of fibre breaking under a stress equal to or less than σ, L the length ratio of the reference length (equals to 1 in this work), σ_0 the characteristic fibre strength, and β_W the Weibull modulus (shape parameter) indicating the dispersion degree of results. Taking the logarithm form of **Eq. (2)**,

$$\ln\ln\left(\frac{1}{1 - F(\sigma)}\right) = \beta_W \ln\sigma - \beta_W \ln\sigma_0, \quad \textbf{(3)}$$

in which the failure probability $F(\sigma)$ comes from

$$F(\sigma) = i/(n+1), \quad \textbf{(4)}$$

where n is the total number of specimens, and i the i^{th} specimen in sort of tensile strength ranked from small to large. As shown in **Fig. 6(a)**, the characteristic strengths of as-received GFs and CNT-g-GFs @ 0.85 wt.%, fitted using the Weibull distribution equation, are 2905 and 2634 MPa, respectively. The slight decrease, by 9.3%, in tensile strength of GFs reveals that the proposed CVD process has minimal impact on the tensile properties of GFs, benefiting from the relatively short synthesis duration (30 min) and low growth temperature (500 °C).

Fig. 6(b) displays the tensile results of laminates with or without a CNT-grafted fibre textile. It can be acquired that there are only slight variations in averaged ultimate tensile strength (0.39%) and Young's modulus (0.96%) of these two sets of laminates, confirming no significant degradation due to sensor integration. The corresponding stress-strain curves acquired in the tensile test are shown in **Fig. S2**.

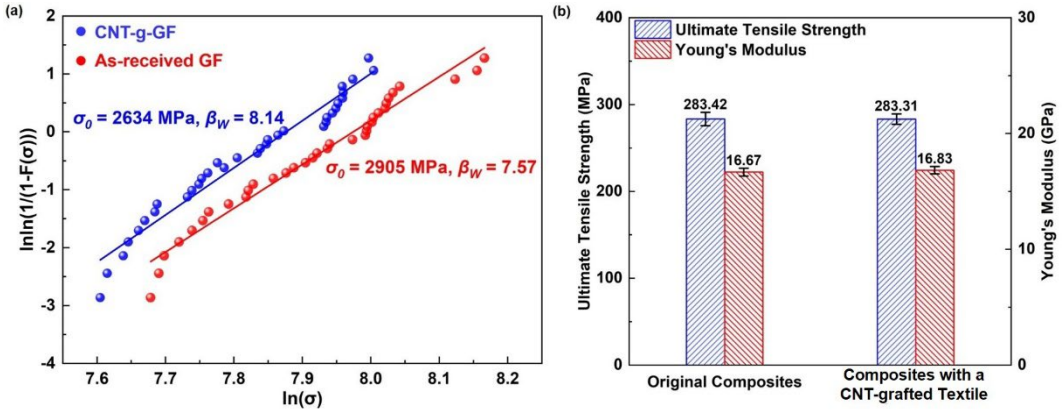

Fig. 6. The Weibull distribution of fracture stress of all tested specimens, with acquired characteristic strengths and Weibull moduli; and (b) averaged tensile moduli and strengths of composites with or without a CNT-grafted textile.

4. Concluding Remarks

In summary, *in situ* grafting of CNTs on GFs is achieved via CVD with a low CNT growth temperature (500 °C), to configure a sensing fibre textile deployed with CNT-g-GF sensors. The high graphitization degree of synthesized CNTs is confirmed via scrutinizing their Raman spectra, with I_d/I_g ratios < 0.89. Through regulating the mass fractions of CNTs, the CNT-g-GF sensors @ 0.85 wt.% demonstrate the highest sensitivity towards GUWs in virtue of the quantum tunnelling effect, with a broad frequency regime from 175 to 375 kHz. Single fibre tensile test (ASTM C1557) reveals the slight degradation, by 9.3%, in single fibre tensile strength due to the exposure to CVD process while the fibre-reinforced polymer matrix composite tensile test (ASTM D3039) confirms no measurable variation in mechanical attributes of hybrid composites owing to the sensor integration.

The proposed integrated functional composites own the great potential in GUW-based integrity monitoring, electromagnetic interference shielding, lighting strike protection, *etc*.

Acknowledgments

This work was supported by General Projects (Nos. 12072141, 51875492, and 61771426) received from the National Natural Science Foundation of China, the National Key R&D Program of China (No. 2022YFB3204300) received from the Ministry of Science and Technology of the People's Republic of China, the Major Scientific Research Project of Zhejiang Lab (No. 113014-AL2201/001), and Zhejiang Provincial Key R&D Program of Zhejiang Province Science and Technology Department (No. 2022C01002). Z Su acknowledges the support from the Hong Kong Research Grants Council via General Research Funds (Nos. 15200922, 15202820 and 15204419), and from Hong Kong Innovation and Technology Commission via project "Smart Railway Technology and Applications" (No. K-BBY1).

References

[1] Y. Su, L. Xu, P. Zhou, J. Yang, K. Wang, L.-m. Zhou, Z. Su, Carbon nanotube-decorated glass fibre bundles for cure self-monitoring and load self-sensing of FRPs, Compos. Commun. 27 (2021) 100899.

[2] A.Y. Boroujeni, M. Tehrani, M. Manteghi, Z. Zhou, M. Al-Haik, Electromagnetic shielding effectiveness of a hybrid carbon nanotube/glass fiber reinforced polymer composite, J. Eng. Mater. Technol. 138(4) (2016).

[3] A. Duongthipthewa, Y. Su, L. Zhou, Electrical conductivity and mechanical property improvement by low-temperature carbon nanotube growth on carbon fiber fabric with nanofiller incorporation, Compos. B. Eng. 182 (2020) 107581.

[4] Y. Wan, W. Hu, B. Yang, X. Zhao, G. Xian, Y. Yuan, L. He, C. Liu, J. Deng, On-line tensile damage monitoring of WGF/epoxy T-joint by the embedded MWCNT@ WGF sensor, Compos. Commun. 23 (2021) 100541.

[5] Z. Wang, B. Yang, G. Xian, Z. Tian, J. Weng, F. Zhang, S. Yuan, X. Ding, An effective method to improve the interfacial shear strength in GF/CF reinforced epoxy composites characterized by fiber pull-out test, Compos. Commun. 19 (2020) 168-172.

[6] D.H. Sung, S.M. Doshi, C. Murray, A.N. Rider, E. Thostenson, Electrophoretic deposition: Novel in situ film growth mechanism of carbon nanocomposite films within non-conductive fabrics for multi-scale hybrid composites, Compos. Sci. Technol. 200 (2020) 108415.

[7] D. He, B. Fan, H. Zhao, X. Lu, M. Yang, Y. Liu, J. Bai, Design of electrically conductive structural composites by modulating aligned CVD-grown carbon nanotube length on glass fibers, ACS Appl. Mater. Interfaces. 9(3) (2017) 2948-58.
[8] K. Yildiz, İ. Gürkan, F. Turgut, F.Ç. Cebeci, H. Cebeci, Fracture toughness enhancement of fuzzy CNT-glass fiber reinforced composites with a combined reinforcing strategy, Compos. Commun. 21 (2020) 100423.
[9] H. De Luca, D. Anthony, E. Greenhalgh, A. Bismarck, M. Shaffer, Piezoresistive structural composites reinforced by carbon nanotube-grafted quartz fibres, Compos. Sci. Technol. 198 (2020) 108275.
[10] J. Sebastian, N. Schehl, M. Bouchard, M. Boehle, L. Li, A. Lagounov, K. Lafdi, Health monitoring of structural composites with embedded carbon nanotube coated glass fiber sensors, Carbon 66 (2014) 191-200.
[11] Z. Zeng, M. Liu, H. Xu, Y. Liao, F. Duan, L.-m. Zhou, H. Jin, Z. Zhang, Z. Su, Ultra-broadband frequency responsive sensor based on lightweight and flexible carbon nanostructured polymeric nanocomposites, Carbon 121 (2017) 490-501.
[12] P. Zhou, X. Yang, Y. Su, J. Yang, L. Xu, K. Wang, L.-m. Zhou, Z. Su, Direct-write nanocomposite sensor array for ultrasonic imaging of composites, Compos. Commun. 28 (2021) 100937.
[13] Y. Su, L. Xu, P. Zhou, J. Yang, K. Wang, L.-m. Zhou, Z. Su, In situ cure monitoring and In-service impact localization of FRPs using Pre-implanted nanocomposite sensors, Compos. Part A Appl. Sci. Manuf. 154 (2022) 106799.
[14] Y. Su, J. Yang, Y. Liao, P. Zhou, L. Xu, L.-m. Zhou, Z. Su, An implantable, compatible and networkable nanocomposite piezoresistive sensor for in situ acquisition of dynamic responses of CFRPs, Compos. Sci. Technol. 208 (2021) 108747.
[15] N. Hu, Y. Karube, C. Yan, Z. Masuda, H. Fukunaga, Tunneling effect in a polymer/carbon nanotube nanocomposite strain sensor, Acta Mater. 56(13) (2008) 2929-36.
[16] R.A. Nandagopal, S. Narasimalu, G. Chai, Study of statistically significant strength degradation of hygrothermal aged CFRP and its weibull analysis, Compos. Commun. 23 (2021) 100566.
[17] J. Dong, C. Jia, M. Wang, X. Fang, H. Wei, H. Xie, T. Zhang, J. He, Z. Jiang, Y. Huang, Improved mechanical properties of carbon fiber-reinforced epoxy composites by growing carbon black on carbon fiber surface, Compos. Sci. Technol. 149 (2017) 75-80.